

Accepted for publication in the Astronomical Journal

Limits on Radio Continuum Emission from a Sample of Candidate Contracting Starless Cores

Daniel W.A. Harvey, David J. Wilner, James Di Francesco¹,
Chang Won Lee², Philip C. Myers

Harvard-Smithsonian Center for Astrophysics, 60 Garden Street, Cambridge, MA 02138

dharvey, dwilner, jdifran, cwlee, pmyers@cfa.harvard.edu

and

Jonathan P. Williams

Department of Astronomy, University of Florida, Gainesville, FL 32611

williams@astro.ufl.edu

ABSTRACT

We used the NRAO Very Large Array to search for 3.6 cm continuum emission from embedded protostars in a sample of 8 nearby “starless” cores that show spectroscopic evidence for infalling motions in molecular emission lines. We detect a total of 13 compact sources in the eight observed fields to 5σ limiting flux levels of typically 0.09 mJy. None of these sources lie within $1'$ of the central positions of the cores, and they are all likely background objects. Based on an extrapolation of the empirical correlation between the bolometric luminosity and 3.6 cm luminosity for the youngest protostars, these null-detections place upper limits of $\sim 0.1 L_{\odot}(d/140 \text{ pc})^2$ on the luminosities of protostellar sources embedded within these cores. These limits, together with the extended nature of the inward motions inferred from molecular line mapping (Lee et al. 2001), are inconsistent with the inside-out collapse model of singular isothermal spheres and suggest a less centrally condensed phase of core evolution during the earliest stages of star formation.

¹currently at the Radio Astronomy Laboratory, University of California, Berkeley, Berkeley, CA 94720-3411; e-mail: jdifran@astron.berkeley.edu

²currently at the Taeduk Radio Astronomy Observatory, Korea Astronomy Observatory, 36-1 Hwaam-dong, Yusung-gu, Taejon 305-348, Korea; e-mail: cw1@hae.trao.re.kr

Subject headings: ISM: globules – ISM: jets and outflows – radio continuum: ISM
— stars: formation

1. Introduction

Star formation occurs within molecular clouds, behind large column densities of obscuring dust that hinders observations of its earliest evolutionary stages. The “Class 0” objects, which are not detected at wavelengths shorter than the submillimeter, represent the youngest protostars observed, with inferred ages of $\sim 10^4$ years (see André, Ward-Thompson & Barsony 1993, André & Montmerle 1994). Even younger protostars need to be identified to improve our understanding of the first stages of protostellar collapse.

The “starless” dense cores, density enhancements within molecular clouds that show no evidence for embedded protostars, may represent an evolutionary stage of the star formation process prior to that of the Class 0 objects. Lee et al. (1999) recently surveyed more than 200 nearby starless cores in spectral lines of dense gas tracers. Seventeen cores were identified with evidence for infalling motions, as suggested by the presence of redshifted self-absorption in line profiles. These rare infall candidates provide an excellent chance to locate the very youngest protostars, whose low luminosity and reddened spectral energy distributions might have escaped detection at far-infrared wavelengths by the Infrared Astronomy Satellite (IRAS).

A possible method to identify extremely young protostellar objects makes use of the well-documented occurrence of simultaneous mass accretion (infall) with mass expulsion (outflow) during star formation. From a sample of 29 Class 0 and Class I protostellar sources, Anglada (1995) noted a strong correlation between 3.6 cm radio continuum luminosity and bolometric luminosity. The radio continuum emission arises from the shock-ionized inner regions of a collimated outflow, while the bolometric luminosity arises predominately from accretion (e.g. Rodriguez et al. 1982, Lada 1985). If outflow is inextricably linked to accretion, the presence of a very young protostar within a so-called “starless core” with evidence for infalling motions can be deduced from the detection of compact radio continuum emission. Using a variant of this concept, Visser (2000) found evidence for three candidate protostars in a sample of 40 Lynds starless cores by detecting high velocity $^{12}\text{CO}(2-1)$ emission from previously unknown outflows.

We present here observations of eight starless cores made with the Very Large Array

(VLA) of the National Radio Astronomy Observatory³ to search for indications of embedded protostars through the detection of compact radio continuum emission from their nascent outflows. The eight cores observed are the nearest objects (< 250 pc) from the survey of Lee et al. (1999) that show redshifted self-absorption in at least two molecular spectral lines.

2. Observations and Data Reduction

The VLA observations of starless cores were made on 1999 March 6 and 1999 April 27 in the D configuration at 3.6 cm (8.46 GHz). The use of the VLA in its most compact configuration and at its most sensitive wavelength maximizes the instrument’s utility for detecting faint sources of radio continuum emission. Table 1 lists the target cores, calibrators, synthesized beam sizes, and the rms noise levels achieved in the images. The central pointing positions for the cores were taken from Lee et al. (1999). The uncertainties in these positions with respect to the column density peaks are at the $\sim 15''$ level. For the March observations of 4 cores at 4–5 hours Right Ascension (in the Taurus region), 3C 48 was used as the flux calibrator (3.15 Jy at 3.6 cm). For the April observations of 4 cores at 15–20 hours R.A. 3C 286 was used as the flux calibrator (5.20 Jy at 3.6 cm). The flux calibration is expected to be accurate to better than 10%. Standard procedures in the AIPS software package were used for all data calibration and imaging.

For each field, sources were located within the 5.3 primary beam half power diameter using the AIPS routine *Search and Destroy*, with a flux threshold of $5\times$ the rms noise in the cleaned image. Table 2 lists the positions and fluxes of the 13 detected sources from the 8 fields. These sources generally fall within the regions of extended molecular line emission, but none are located within $1'$ of the adopted positions for the column density peaks. This choice of criterion for positional coincidence is arbitrary, but it is likely that all the detected sources are background objects. Nevertheless, more millimeter/sub-millimeter observations must be done to locate the column density peaks with better accuracy, to substantiate the significance of the observed displacements. It remains conceivable that one or more of the 3.6 cm sources may be tracing smaller clumps of material embedded within the cores; this possibility could be tested by future higher resolution observations. The observed source counts are consistent with expectations for a background population. Based on a detection threshold of 0.09 mJy, the source properties from Condon (1984), and the calculation in the appendix of Anglada et al. (1998), on average 1.0 background sources are expected per

³The National Radio Astronomy Observatory is operated by Associated Universities Inc., under contract with the National Science Foundation.

field, for a total of 8 ± 3 sources, which is consistent within 2σ of the detected number. For the strongest source, L1521F (1), a reliable match is found in the NRAO VLA Sky Survey (NVSS) point source catalog. The NVSS flux measurement at 21 cm (1.4 GHz) implies a radio spectral index for this source of -0.70 ± 0.02 , which suggests synchrotron emission from a background radio galaxy. This source is also the only resolved member of the sample (the resolution of the cleaned images is $\sim 10''$). The remaining unresolved sources show no matches in the SIMBAD astronomical database.

3. Discussion

3.1. Bolometric Luminosity Limits

The lack of positional coincidence between any of the detected radio continuum sources and the centers of the starless cores suggests that none of these sources are associated with the cores. Hence, the observations allow us to place upper limits on the 3.6 cm radio continuum luminosity of any compact sources present in the cores, and thus, upper limits on their bolometric luminosities following Anglada (1995). Figure 1 shows the radio continuum and bolometric luminosity data for the 29 sources compiled by Anglada, together with a least-squares fit. The fitted correlation

$$\log [S_{3.6\text{ cm}} d^2 \text{ (mJy kpc}^2)] = (-2.1 \pm 0.1) + (0.7 \pm 0.1) \log [L_{\text{bol}} (L_{\odot})]$$

allows the observed trend to be extrapolated to lower luminosities, the regime of our sensitive VLA observations. While there is no observational support for the validity of this extrapolation, there are no changes expected in the relevant mechanisms at lower luminosity levels that would suggest a breakdown of the correlation.

For the 4 Taurus cores (L1521F, TMC2, TMC1, CB23) at a distance of 140 pc (Elias 1978), the correlation and 5σ upper limits on the radio continuum luminosity imply bolometric luminosity limits of $L \lesssim 0.1 L_{\odot}$. For the three Ophiuchus cores (L183, L158, L234E-S) at a distance of 165 pc (Chini 1981), the implied limits are $L \lesssim 0.2 L_{\odot}$. For L694-2, at an assumed distance of 250 pc that derives from an association with the cloud complex harboring the B335 core (Tomita, Saito & Ohtani 1978), the implied bolometric luminosity limit is $L \lesssim 0.7 L_{\odot}$. Figure 1 shows the upper limits for the 3.6 cm luminosities as arrows. The uncertainty in these limits due to the uncertainty in the fitted correlation is $\sim 50\%$.

3.2. Comparison with IRAS Limits

In some circumstances, the limits on protostar luminosity implied by the VLA null-detections represent a substantial improvement on limits implied by the lack of an IRAS point source. For objects like starless cores that may be characterized by low temperatures, the limit from the longest wavelength IRAS band (100 μm) most strongly constrains luminosity. For isolated objects at high Galactic latitudes ($|b| > 50^\circ$), the IRAS Point Source Catalog has a 50%-completeness limit of 1.0 Jy at 100 μm (Beichman et al. 1988). Nearer to the plane of the Galaxy, in more complicated regions such as Ophiuchus or Orion, the limits are often much higher due to extended “Cirrus” emission, and confusion with other sources. For example, VLA 1623, the prototypical Class 0 object, escaped detection by IRAS despite a fairly warm dust temperature ($T \simeq 20$ K) and substantial bolometric luminosity $L \sim 0.5$ – 2.5 L_\odot (Andr , Ward-Thompson & Barsony 1993). For this core, crowding with nearby sources causes the IRAS limiting flux to be raised to 45 Jy (Ward-Thompson 1993).

To calculate appropriate IRAS limits on bolometric luminosity, we assume that the spectral energy distributions of Class 0 objects and dense cores may be modeled reasonably well by modified graybodies of the form:

$$F_\nu = B_\nu(T_{dust})(1 - \exp[-\tau_\nu])\Omega_S ,$$

where $B_\nu(T_{dust})$ denotes the Planck function at frequency ν for a dust temperature T_{dust} , τ_ν is the dust optical depth, and Ω_S the solid angle subtended by the source (Gordon 1988, Ward-Thompson, Andr  & Kirk 2001). The optical depth is proportional to the mass opacity of the dust, which is generally assumed to follow a power law with frequency. The power law index is uncertain for the dust in dense cores, but bounded to a small range (Ossenkopf & Henning 1994). Here, we adopt $\tau_\nu \propto \nu^{1.5}$, as found for VLA 1623 by Andr  et al. 1993. The solid angle subtended by the source is constrained to be $\lesssim 2'$ in diameter, the resolution of IRAS at 100 μm . The maximum bolometric luminosity of such a graybody that may be hidden below a 1.0 Jy IRAS completeness limit is temperature dependent, roughly 1 L_\odot for $T_{dust} = 10$ K, and falling to 0.1 L_\odot for $T_{dust} = 14$ K, for a source at Taurus distance that is optically thin for $\lambda \gtrsim 100$ μm . This result is similar to the 0.05–0.1 L_\odot limit for Taurus obtained by Myers et al. (1987), although the analysis presented here is more applicable to Class 0 objects.

Since the cores in this study are often viewed superposed against a parent molecular cloud, the 100 μm point source completeness limit may be worse than the nominal value of 1 Jy for isolated objects. For a ~ 3 Jy limit, a source as bright as 0.3 L_\odot at 140 pc would have been undetected by IRAS even with a dust temperature of 14 K. The presence of even a small amount of (visible) warm dust would strongly increase the emission at the shorter

wavelengths, and substantially lower the bolometric luminosity that could be hidden from IRAS. But such warm dust would be located close to the protostar, in the central regions of the core, in which case the solid angle subtended by the warm component would be small, and it would be shielded from view by absorption in the intervening layers of cold dust. To illustrate this scenario, consider an example of a cold core (14 K) that surrounds a warm dust component (40 K) that represents $\sim 1\%$ of the total dust mass. If this core has an optical thickness that is only one-tenth that of VLA 1623, making it optically thick for $\lambda \lesssim 20 \mu\text{m}$, then it could produce a bolometric luminosity of $0.1 L_{\odot} (d/140 \text{ pc})^2$ but remain undetected by IRAS with a $100 \mu\text{m}$ detection limit of $\sim 3 \text{ Jy}$. In these circumstances, the limits on protostar luminosity implied by the VLA null-detections are at least comparable to, and in many cases significantly lower than the corresponding IRAS limits.

3.3. Implications for the Infall Process

The null-detection of an embedded point source in a contracting core has implications for the nature of the infall process. Tafalla et al. (1998) presented a detailed discussion of these implications pertaining to L1544, a starless core in Taurus with evidence for infalling motions and comparable 3.6 cm radio continuum limits (Williams et al. 1999). In short, the low luminosities and extended sizes of the observed regions of inward motions are inconsistent with the widely applied model of inside-out collapse of a singular isothermal sphere (Shu 1977). In this model, collapse leads to the formation of a central point source with luminosity $L \sim a^6 t / G R_*$, where a is the effective sound speed, t is the time since the onset of collapse, and R_* is the protostellar radius (Shu, Adams, & Lizano 1987). Taking $R_* \simeq 3 R_{\odot}$ (Stahler 1988) and $a \simeq 0.19 \text{ km s}^{-1}$ ($T \simeq 10 \text{ K}$), the model predicts $L \sim 3 (t/10^5 \text{ yr}) L_{\odot}$. Infall onto a disk would reduce this luminosity (Kenyon et al. 1993), but these very young objects undetected by IRAS show no evidence for disks, nor are large disks predicted at such early times (Terebey, Shu & Cassen 1984). In the context of the Shu model, and using the Anglada correlation between radio continuum luminosity and bolometric luminosity, for an embedded source at Taurus distance to remain undetected by our VLA observations would require $t \lesssim 4 \times 10^3$ years, corresponding to an infall radius of only $R_{\text{inf}} \lesssim 8 \times 10^{-4} \text{ pc}$. For a source at Ophiuchus distance, the corresponding values are $t \lesssim 7 \times 10^3$ years, and $R_{\text{inf}} \lesssim 1 \times 10^{-3} \text{ pc}$, while at the greater distance of L694–2, the values are $t \lesssim 2 \times 10^5$ years, and $R_{\text{inf}} \lesssim 0.04 \text{ pc}$. Lee et al. (2001) have computed sizes for the infalling regions in six of the eight cores that were observed in this study (TMC2, TMC1, L183, L158, L234E–S, and L694–2) by analyzing the extent of redshifted self-absorption in lines of CS and N_2H^+ . The infall radii so derived range from 0.07 pc for L158 up to 0.17 pc for TMC1, and are typically 0.1 pc. The method used to calculate these radii is fairly simple, and more detailed modelling

may refine the exact values. Nevertheless, the observed infall radii are very much larger than the limits on radii derived from the strict luminosity constraints found here assuming the inside-out collapse scenario. Moreover, the ambipolar diffusion process in a strongly sub-critical core apparently cannot explain the high velocities of infalling material observed in these cores (Lee et al. 2001; Ciolek & Mouschovias 1995). The cores studied here represent a sample whose inward motions are inconsistent with the standard theories of low mass star formation.

4. Summary

We used the VLA to search for 3.6 cm radio continuum emission from embedded outflows in eight “starless cores” that show evidence for infalling motions in the profiles of molecular spectral lines (Lee et al. 1999). We detected a total of 13 compact sources of radio continuum emission. None of the sources are within an arcminute of the column density peaks, and the source counts are consistent with expectations for a background population. Based on these apparent null-detections and an observed correlation between outflow luminosity and bolometric luminosity from protostellar objects, we place approximate upper limits on the luminosities of any embedded protostars (with uncertainty $\sim 50\%$) of $\lesssim 0.1 L_{\odot}(d/140 \text{ pc})^2$. These limits, together with the extended nature of the inward motions inferred from molecular line mapping (Lee et al. 2001), are inconsistent with the inside-out collapse model of singular isothermal spheres and suggest a less centrally condensed phase of core evolution during the earliest stages of star formation.

This research has made use of the SIMBAD database, operated at CDS, Strasbourg, France.

REFERENCES

- André, P., & Montmerle, T. 1994, ApJ, 420, 837
- André, P., Ward-Thompson, D., & Barsony, M. 1993, ApJ, 406, 122
- Anglada, G., Villuendas, E., Estalella, R., Beltrán, M.T., Rodríguez, L.F., Torrelles, J.M., & Curiel, S. 1998, AJ, 116, 2953
- Anglada, G. 1995, RMxAA, 1, 67
- Beichman, C. et al. 1988, *Infrared Astronomical Satellite (IRAS) Catalogs and Atlases, vol. 1, Explanatory Supplement*, NASA RP-1190 (Washington, DC: GPO)
- Chini, R. 1981, å, 99, 346
- Ciolek, G.E. & Mouschovias, T.CH. 1996, ApJ, 468, 749
- Condon, J.J. 1984, ApJ, 287, 461
- Elias, J.H. 1978, ApJ, 224, 857
- Gordon, M.A. 1988, ApJ, 331, 509
- Kenyon, S.J., Calvet, N. & Hartmann, L. 1993, ApJ, 414, 676
- Lada, C.J. 1985, ARA&A, 23, 267
- Lee, C.W., Myers, P.C., & Tafalla, M. 2001, ApJS, 136, 703
- Lee, C.W., Myers, P.C., & Tafalla, M. 1999, ApJ, 526, 788
- Myers, P.C., Fuller, G.A., Mathieu, R.D., Beichman, C.A., Benson, P.J., Schild, R.E., & Emerson, J.P. 1987, ApJ, 319, 340
- Ossenkopf, V. & Henning, T. 1994, A&A, 291, 943
- Rodríguez, L.F., Carral, P., Moran, J.M., & Ho, P.T.P. 1982, ApJ, 260, 635
- Shu, F.H. 1977, ApJ, 214, 488
- Shu, F.H., Adams, F.C., & Lizano, S. 1987, ARA&A, 25, 23
- Stahler, S.W. 1988, ApJ, 332, 804
- Tafalla, M., Mardones, D., Myers, P.C., Caselli, P., Bachiller, R., & Benson, P.J. 1998, ApJ, 504, 900
- Terebey, S., Shu, F.H. & Cassen, P. 1984, ApJ, 286, 529
- Tomita, Y., Saito, T. & Ohtani, H. 1979, PASJ, 31, 407
- Visser, A. 2000, Ph.D. thesis, University of Cambridge (UK)
- Ward-Thompson, D. 1993, MNRAS, 265, 493
- Ward-Thompson, D., André, P. & Kirk, J.M. 2001, MNRAS, *in press*

Williams, J.P., Myers, P.C., Wilner, D.J. & Di Francesco, J. 1999, ApJ, 513, L61

Table 1. Dense Cores Observed at 3.6 cm

Source	Phase Center		Calibrator	Beam ("×")	RMS Noise (μ Jy)
	α (J2000)	δ (J2000)			
L183	15 ^h 54 ^m 06 ^s .5	−02° 51′ 39″	1543 − 079	11.6 × 9.8	15
L158	16 47 23.2	−13 59 21	1543 − 079	13.5 × 9.8	16
L234E-S ...	16 48 08.6	−10 57 24	1707 + 018	12.9 × 9.9	18
L694-2	19 41 04.5	+10 57 02	1950 + 081	11.9 × 9.1	20
L1521F	04 28 39.8	+26 51 35	0432 + 416	10.3 × 9.1	22
TMC2	04 32 48.7	+24 24 12	0432 + 416	10.4 × 9.1	18
TMC1	04 41 33.0	+25 44 44	0432 + 416	10.4 × 9.1	17
CB23	04 43 31.5	+29 39 11	0432 + 416	10.3 × 9.1	18

Table 2. Sources Detected at 3.6 cm

Source	Position ^a		Flux ^b (mJy)	Angular Displacement ^c ($''$)
	α (J2000)	δ (J2000)		
L158 (1)	16 ^h 47 ^m 16 ^s .7	−14° 00′ 57 $''$	0.27	135
(2)	16 47 24.0	−14 01 15	0.37	115
L234E–S (1) . . .	16 48 05.0	−10 59 20	0.55	128
(2) . . .	16 48 06.5	−10 56 07	0.25	83
L694–2 (1)	19 40 57.2	+10 57 30	2.60	111
L1521F (1)	04 28 41.2	+26 53 55	10.75	142
TMC2 (1)	04 32 42.6	+24 23 24	0.24	96
(2)	04 32 54.2	+24 22 43	0.13	116
TMC1 (1)	04 41 25.4	+25 42 53	0.67	151
(2)	04 41 25.7	+25 43 49	0.75	113
(3)	04 41 39.0	+25 43 24	0.36	114
CB23 (1)	04 43 34.9	+29 38 05	0.14	79
(2)	04 43 35.0	+29 37 13	0.26	127

^aPosition errors are $\sim 1''$

^bCorrected for primary beam attenuation

^cFrom Phase Center in Table 1

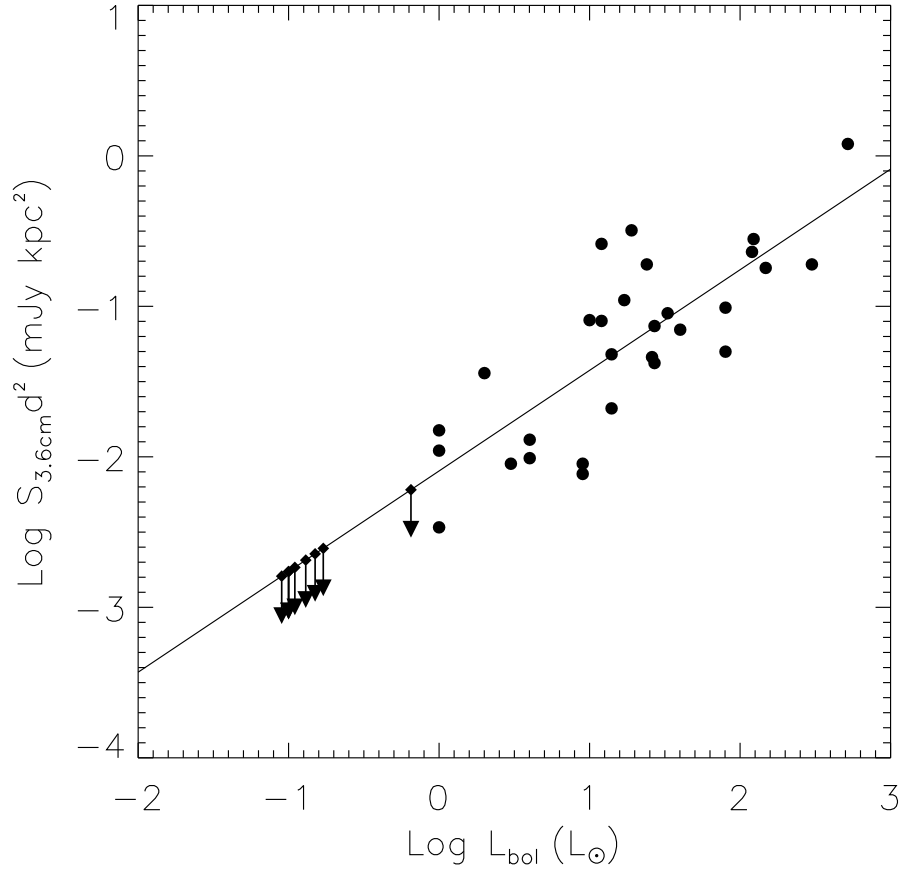


Fig. 1.— Log-log plot of 3.6 cm luminosity against bolometric luminosity for 29 outflow sources from Anglada (1995). A linear least-squares fit ($r=0.79$) indicated by the line has been used to extrapolate the observed trend to the sensitivity of our VLA observations. The fitted line has been used to calculate approximate upper limits on the bolometric luminosity of any protostar that might remain undetected in our observations. These upper limits are marked with arrows.